Energy Transfer Study of the Cylindrical Interface Formed by Asymmetric Isoprene−Methyl Methacrylate Diblock Copolymers Bearing a Dye at the Junction

Jian Yang, Xudong Lou, John G. Spiro, and Mitchell A. Winnik*

Department of Chemistry, University of Toronto, 80 St. George Street, Toronto, Ontario, Canada M5S 3H6

Received September 22, 2005; Revised Manuscript Received January 6, 2006

ABSTRACT: The experiments described here were designed to determine the characteristic width δ of the cylindrical interface in a block copolymer that forms a hexagonal phase in the bulk state. We used fluorescence resonance energy transfer (FRET) to study films consisting of mixtures of donor- and acceptor-labeled poly(isoprene-*b*-methyl methacrylate) (PI−PMMA, 29 vol % PI). Dye labels were attached at the PI−PMMA junctions. Because the dyes are connected to the junctions, they are confined to the block copolymer interface. To obtain information about the width of the interface separating the components, we compared measured and simulated donor fluorescence decay profiles. We developed a Monte Carlo method to introduce donor and acceptor sites within the interface and then used this dye distribution to calculate simulated "experimental" decay profiles. In this way we were able to examine the appropriateness of using a preaveraged value of the orientation parameter in evaluating FRET data. We found that a value of $\langle|\kappa|\rangle^2 = 0.40$ gave a reasonable agreement with results obtained by considering random orientation of dipoles for each donor−acceptor pair. Through these experiments, we found a value of δ slightly smaller than 1.0 nm, confirming that PI and PMMA are very meagerly miscible polymers.

Introduction

Diblock copolymers consisting of two immiscible or weakly miscible components undergo microphase separation in the melt state. Phase separation occurs for polymers in which the product of its chain length N and the Flory−Huggins interaction parameter χ_{FH} exceeds a critical value.[1] If the polymer samples have a uniform composition, they self-assemble to form periodic structures. The structures formed can have different morphologies (spheres, cylinders, gyroids, lamellae), depending on the volume fraction of the blocks and the magnitude $\chi_{FH}N$. The individual microphases are separated by even thinner interfaces, which have a characteristic thickness δ larger than the size of individual monomer units but much smaller than the radius of gyration of the component polymer chains. Because of the small domain size of the periodic structure, knowledge about the interface between the two block phases becomes important in understanding and predicting properties of block copolymers in the bulk state.

Polymer interfaces are difficult to study because of their small scale. For planar samples of polymer blends and for symmetrical diblock copolymers in which the microphase-separated lamellae can be oriented parallel to the plane of the substrate, specular neutron reflectivity (SNR)[2−4] measurements provide rich information about the polymer concentration gradient across the interface. To obtain contrast, this experiment requires one of the blocks (or for blends, one of the components) to be deuterated. One cannot obtain the polymer segment density directly form the reflectivity plots. Rather, one combines the theory of neutron reflectivity with the theory of polymer interfaces to find the parameters that give the best agreement between simulated and experimental data. The data analysis is somewhat complicated by the contribution of capillary waves to the measured signal. It is difficult to distinguish this waviness from the intrinsic polymer segment distribution profile, but the experiment provides raw data with good accuracy and high precision.

Fluorescence resonance energy transfer (FRET)[5−7] measurements have also been used to study the interfaces for diblock copolymer lamellae. This experiment requires pairs of polymers of nearly identical composition and length: one labeled at the junction with a donor dye (D) and the other labeled at the junction with an acceptor dye (A). The dyes monitor the locus of the junctions, which defines the span of the interface. FRET experiments provide a measure of the distribution of D and A groups across the interface. In a FRET experiment, one measures donor fluorescence decay profiles for mixtures of D- and A-labeled block copolymers. As is the case for SNR experiments, one cannot obtain the junction distribution directly from this decay profile. Rather, one has to carry out simulations of the experiment, combining the theory of energy transfer in restricted geometry[8,9]with the theory of polymer interfaces to find the parameters that give the best agreement between simulated and measured data. To analyze the experimental data, one needs independent knowledge of the characteristic (Förster) distance R_0 for energy transfer between D and A, the orientation parameter κ^2 that contributes to the energy transfer rate, and an independent measurement of the lamellar spacing. We have reported FRET studies on the lamellar interface formed by symmetrical samples of PI−PMMA[7,10] and poly(styrene-*b*-methyl methacrylate) (PS−PMMA).[11] In our experience with lamellar systems, the precision of the FRET experiment is comparable to that of SNR, and the FRET experiment on diblock copolymers operates over too short a length scale to be sensitive to capillary waves in the interface.

Recently, there has been strong interest in block copolymers that self-assemble in the bulk to yield a hexagonal array of cylinders. These systems, for example, can serve as templates for the formation of periodic arrays of hollow pores. There are very few studies of polymer interfaces in block copolymer cylinders. This is a system in which FRET experiments should

* To whom correspondence should be addressed.

10.1021/ma052068a CCC: $33.50
Published on Web 02/24/2006

Table 1. Characteristics of Asymmetric PI−PMMAs

polymers	M_n(GPC)[a]	dye attached fraction (x_{dye})[b]	PDI[a]	V_{PI}:V_{PMMA}[c]	M_n-PI(GPC)[a]	PDI[a]
PI-9Phe−PMMA	37 000	0.96	1.04	29:71	10 400	1.05
PI-2An−PMMA	37 000	1.0	1.04	29:71	10 100	1.05

[a] Relative to PMMA standards. [b] The fraction of polymer labeled with dye, assuming that the diblock copolymers and their corresponding model compounds (see ref 7) have the same molar extinction coefficient. [c] Calculation based on ^{1}H NMR analysis.

be particularly useful. As in the case of lamellar systems, the D- and A-dyes of junction-labeled block copolymers serve as markers for the distribution of the block junctions across the interface.

The description of FRET in a restricted cylindrical geometry is much more complicated than the corresponding description for planar and spherical geometries. An analytical solution to this problem has been proposed recently by Farinha et al.[12] We recently developed an alternative data analysis method for FRET in restricted geometries based on Monte Carlo (MC) calculations.[13,14] This methodology focuses on simulating the spatial distribution of the donors and acceptors in the restricted geometry. The extent of energy transfer can be calculated on the basis of loci of the chromophores. The most attractive advantage of this methodology is that one can selectively choose the dipole orientation for each pair of chromophores to study its effect on the rate and extent of energy transfer in the confined geometries. In analytical approaches to the evaluation of FRET data, one has to assume a preaveraged value for the orientation term $\langle|\kappa|\rangle^2$. When the MC and analytical methods were compared for the analysis of donor decay profiles for junction-labeled symmetrical PI−PMMA block copolymers, which form a periodic lamellar structure, the two approaches yielded identical values of δ, provided that an appropriate value of $\langle|\kappa|\rangle^2$ was employed in the data analyses.

In this paper, we describe FRET measurements on polymer films formed by a pair of dye-labeled asymmetric PI−PMMA diblock copolymers (29 vol % PI) that form a hexagonal phase consisting of cylindrical PI cores in a PMMA matrix. The polymers are labeled at the junction with either a phenanthrene (donor) group or an anthracene (acceptor) group, and thus the dyes are confined to the interface between the two block phases. We use a MC-based analysis of the energy transfer between the labeled donors and acceptors in films formed by mixtures of the two diblock copolymers to evaluate how effectively the thickness of the interface between PI cylinders and the PMMA matrix can be retrieved.

The paper is organized as follows: after the Experimental Section, we present a detailed description of the use of the MC methodology to construct models for the locus of the dyes in the interface and the theory of fluorescence decay simulations and analyses based on those loci. Next, we describe small-angle X-ray scattering (SAXS) and FRET experiments on the asymmetric, dye-labeled PI−PMMA samples. Finally, we show how these simulations can be used to calculate a value for the interface thickness and comment on the strengths and limitations of this methodology.

Experimental Section

Instrumentation. UV−vis absorption spectra were recorded on a Perkin-Elmer Lambda 25 UV/vis spectrophotometer. Molecular weights (M) and molecular weight distributions (MWD) were determined by gel permeation chromatography (GPC, Viscotek VE2100), using THF as the eluent and PMMA as molecular weight standards. Signals were monitored using tandem UV−vis (UV) and refractive index (RI) detectors. For the UV detector, the absorption wavelengths were 300 nm for phenanthrene and 370 nm for anthracene. Fluorescence spectra were measured with a Fluorolog 3 luminescence spectrometer from JY Horiba. Small-angle X-ray scattering (SAXS) measurements were performed on a NanoStar X-ray camera from Bruker AXS GmbH. The instrument was operated with the Cu Kα line (λ = 0.154 nm) and a sample-to-detector-distance of 62.85 cm. The scattering patterns were recorded with the Hi-Star 2-D X-ray detector. Azimuthal integration from 0° to 360° was used to extract the q dependence of the scattering intensity. Solution ^{1}H NMR spectra were recorded on a Unity 400 NMR spectrometer at room temperature, with chemical shifts quoted in ppm. Fluorescence decay profiles were measured using a single photon timing instrument from IBH with a pulsed flash lamp (0.5 atm of D_2) as an excitation source.[15] The time scale was set to 0.907 ns per channel.

Table 2. Mole Fractions of Phe and Concentrations of An in the Polymer Films

sample no.	1	2	3	4	5
f_{Phe}[a]	1	0.84	0.77	0.66	0
C^0_{An} (mM)[b]	0	4.58	6.70	10.0	29.4

[a] Calculated from $f_{Phe} = x_{Phe}m_{PI-9Phe-PMMA}/(x_{Phe}m_{PI-9Phe-PMMA} + x_{An}m_{PI-An-PMMA})$, where m refers to the number of moles of each component. [b] Calculated from the mole number of An ($m_{PI-An-PMMA}$), the degree of labeling (x_{An}), the mean number-averaged molecular weight (M_n) of the polymer, and the average polymer density (ρ), $C^0_A = x_{An}m_{PI-An-PMMA}/(M_n\rho)$.

Polymer Synthesis and Characterization. Asymmetric donor (phenanthrene)-labeled and acceptor (anthracene)-labeled PI−PMMAs were synthesized following the procedure described previously.[7,16] In both of the polymer syntheses, isoprene was polymerized anionically in tetrahydrofuran and then end-capped with a 1-aryl-1-phenylethylene derivative. The anion formed was used subsequently to initiate MMA polymerization. For the donor-labeled polymer, the aryl group was 9-phenanthryl (9Phe). For acceptor-labeled polymer, the aryl group was anthracene attached via the 2-position (2An). A small amount of PI homopolymer was taken out of the reaction after the polymerization of isoprene to measure the molecular weight of the PI block. GPC traces of the two asymmetric PI−PMMA samples show that the dyes are attached to the diblock copolymer chain, and no free dyes were observed in the final products. UV−vis and emission spectra of both diblock copolymers are very similar to those of corresponding symmetric dye-labeled PI−PMMA block copolymers described in ref 16. The two blocks have a volume ratio of 29:71 (PI:PMMA; ^{1}H NMR). The dye content of each diblock copolymer was calculated from its UV absorption under the assumption that the dye-labeled PI−PMMA and its corresponding dye model compound have the same extinction coefficient in THF solution.[17] Table 1 shows the characteristics of the two diblock copolymers.

Sample Preparation. Samples of asymmetric PI-9Phe-PMMA and PI-2An-PMMA were each dissolved in tetrahydrofuran (reagent grade, Aldrich), to form 10 wt % solutions. These solutions were mixed to give solutions with different weight ratios of the two polymers (PI-9Phe-PMMA/PI-2An-PMMA). The solutions were transferred into craters (length: 2.0 cm; width: 1.0 cm; depth: 0.2 cm) cut into a Teflon mold. These samples were dried very slowly at room temperature in a box equipped with small release holes in the presence of a reservoir containing additional THF solvent in order to minimize the drying rate. In this way we obtained smooth, transparent, free-standing films (Table 2) for the energy transfer study. All the samples were annealed at 130 °C under vacuum for 5 h. For SAXS measurements, only films of the two neat diblock

copolymers (samples 1 and 5) were examined. SAXS and FRET measurements were performed at room temperature.

Time-Resolved Fluorescence Intensity Decay Measurements. Fluorescence decay profiles of the polymer films were measured at room temperature. The samples were excited at $\lambda_{ex} = 300$ nm, and the phenanthrene fluorescence was detected at $\lambda_{em} = 350$ nm. A band-pass filter (350 ± 5 nm) was used to remove emission from anthracene. The instrument response function, used for the convolution analysis, was obtained by exciting a solution of *p*-terphenyl in deaerated cyclohexane (lifetime: 0.96 ns). The film was held in a quartz tube, and the position was adjusted to eliminate the scattering effect of the excitation beam. In each experiment, 10 000 counts were collected in the maximum channel.

Monte Carlo Calculations and Data Analysis Methodology

Generating the Loci of the Donor and Acceptor Dyes. In ref 13 we presented a detailed description of a Monte Carlo method for the generation of dye loci in confined geometries. The main idea of this algorithm is to generate points in space that can later be identified as the loci of donor and acceptor dyes and which satisfy the spatial distribution associated with the confined geometries as well as the dye concentration in the experimental system. FRET between donors and acceptors can then be studied on the basis of those loci. In this section, we describe a use of this algorithm to simulate the spatial dye distribution across the cylindrical interface formed by our dye-labeled PI−PMMA samples.

These samples each have a chromophore (donor or acceptor) attached at the junctions of the PI and the PMMA blocks. As a consequence, the chromophores are confined to the interface between the PI cylinders and PMMA matrix when the diblock copolymers self-assemble in bulk. The spatial distribution of D and A groups across the interface can be represented by the distribution of the block junctions. According to Helfand−Tagami mean-field theory,[18−20] the modified junction distribution density $P(r - r_{core})$ across the interface is given by the expression

$$P(r - r_{core}) = r\,\mathrm{sech}\left[\frac{2(r - r_{core})}{\delta}\right] \quad (1)$$

where δ is the interface thickness, r is the radial distance, starting from the center axis of the PI cylinder, and r_{core} is the radius of the PI cylinder (6.8 nm, as determined by SAXS).

Figure 1 shows a sketch of the hexagonal structure formed by the asymmetric PI−PMMA. As shown in the figure, a hexagonal cell (lateral length: L; height: L_Z) contains a PI cylinder (radius: r_{core}; height: L_Z) in the center. On the basis of this model hexagonal structure and the spatial distribution of the dyes (eq 1), we simulated the dye (donor and acceptor) loci in an off-lattice space by the MC method, in which we treated all chromophores as points.[21] We considered a single hexagonal cell and assumed that energy transfer can occur only within a single hexagonal cell.[22] All dyes are located in a diffuse tubelike interface between the PI cylinder and the PMMA matrix. The number of dyes (N^0_{dye}) placed in the hexagonal cell was calculated from the bulk concentration (C^0_{dye}) of donors and acceptors in the polymer sample and the volume of the hexagonal cell (V_{HEX})

$$N^0_{dye} = N_{AV} C^0_{dye} V_{HEX}$$
$$V_{HEX} = \sqrt{3} D^2 L_Z/2 \quad (2)$$

where N_{AV} is the Avogadro constant and the subscript "dye" represents the donors or acceptors. D is the center-to-center distance of the PI cylinders ($D = 24$ nm, determined by SAXS, see below). In all calculations, the height of the hexagonal cell, L_Z, was set to 500 nm, and periodic boundary conditions were applied in this direction. We also fixed the bulk concentration of donors at 5 mM (a total of 750 donors in the model diffuse interface per 500 nm in height) to simplify the calculation.[23]

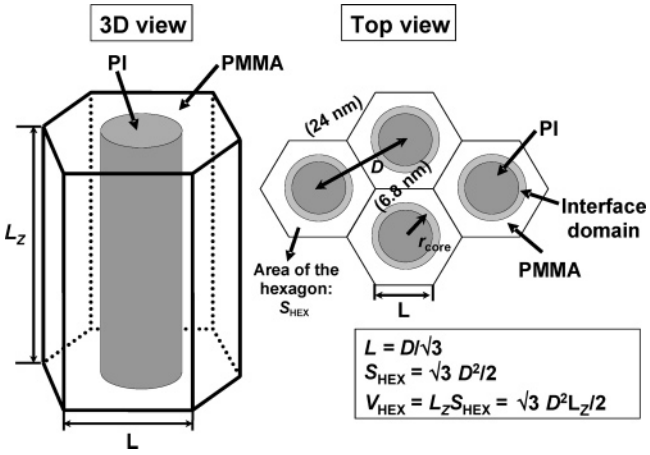

Figure 1. 3D and top-view images of the hexagonal structure formed by the asymmetric PI−PMMA samples. As indicated in the figure, the gray areas represent the PI domains and the white parts in the hexagons denote the PMMA phase. The gradient between the two phases represents the interface. The values characterizing the structure were determined by SAXS and ^{1}H NMR measurements: correlation distance ($D = 24$ nm) between the PI cylinders; radius ($r_{core} = 6.8$ nm) of the PI cylinders. Other parameters include L, lateral length of the hexagonal cell; S_{HEX}, the cross-sectional area of the hexagonal cell; L_Z, the height of the hexagonal cell. V_{HEX} is the volume of the hexagonal cell.

To obtain the spatial distribution of the dyes across the interface, we placed the dyes in the diffuse tubelike interface into the lateral surfaces of many concentric cylinders, with their radii increasing from $r_1 = 0.0$ nm to $r_{121} = D/2$, in steps of 0.1 nm. ($r_1 = 0.0$ nm corresponds to a degenerate cylinder, the common axis.) The dyes within each cylinder are considered to be randomly and homogeneously distributed. The number of dyes (donors or acceptors), $N_{dye}(r_i - r_{core})$,[24] in each cylinder was calculated by

$$N_{dye}(r_i - r_{core}) = N^0_{dye} P(r_i - r_{core}) / \sum_{i=1}^{i=121} P(r_i - r_{core}) \quad (3)$$

where $P(r_i - r_{core})$ is the spatial dye distribution described in eq 1. For each cylinder we calculated the number of dyes to be incorporated and then introduced these dyes randomly within the cylinder. By summing over all cylinders, we are able to generate the dye loci for the sample at a certain acceptor concentration and a certain assumed value of interface thickness. We constructed these models for the three donor + acceptor samples listed in Table 2 (samples 2−4). For each sample, a series of model systems were constructed with interface thickness values δ ranging from 0.2 to 2.0 nm (in steps of 0.1 nm). In each model system, to minimize the data fluctuation associated with the MC method, we performed five parallel generations of dye loci, each of which was used to calculate a delta-function excitation fluorescence decay curve for the same model system (eq 4 or eq 6, see below). These five decays were then averaged at each time channel to give an average decay curve, which was then used to fit the experimental decay (see the following section). Figure 2 shows an example of the spatial distribution of acceptors in the model system with a value of

the interface thickness of $\delta = 1.0$ nm at $C_{An}^0 = 4.58$ mM (sample 2).

We remind the reader that the simulation does not take into account the space occupied by the dyes at the block copolymer junction, and the points that represent the dye refer in fact to the positions of the centers of their transition dipoles. The An and Phe dyes are planar objects that occupy a volume approximately $10 \times 7 \times 3$ Å. The density of the dyes is low enough that the interaction between dyes does not contribute to the calculation. In another system, this effect was tested by deleting from the calculation dye pairs within 1 nm, without any consequences to the computed values.[13]

PI and PMMA are strongly immiscible polymers. We will find from the analysis described below that the width of the interface is on the order (1 nm) of the length of the long axis of the individual dyes. From this perspective, a reviewer raised a question about dye orientation in the system. Both self-consistent-field theory and simulations of polymer blends indicate that the overall density profile normal to the interface will pass through a minimum.[25] This may suggest that the dye moieties will orient themselves in such a way that they will be mostly in the low-density region(s). The reviewer asks if this might not lead to the dyes orienting themselves with their long axes parallel to the plane of the interface. This point is relevant to the orientation parameter used in the analysis of FRET data.

We have tried in previous studies to address the issue of possible nonrandom dye orientation. Monte Carlo simulations of block copolymer chains[14,26] showed that there was no detectable preference for the chain backbone orientation with respect to the plane of the interface. Experiments in which the position of the attachment of the An dye to the chain backbone at the junction between the blocks was varied had no effect, for PI−PMMA lamellae, on the interface width determined in FRET experiments.[10] While we cannot rule out absolutely possible orientation effects in energy transfer between the donor and acceptor dyes, all evidence in hand points to a random orientation of transition dipoles in the system.

Fitting FRET Data To Obtain the Interface Thickness. In the preceding section, we described the generation of the loci of donors and acceptors in a model geometry corresponding to the junction distribution for a cylindrical diblock copolymer structure. On the basis of these loci, delta-function excitation fluorescence decays could be calculated by[27]

$$I(t) = \frac{I_0}{N_D^0} \exp\left(-\frac{t}{\tau_D}\right) \sum_{j=1}^{N_D^0} \exp\left(-t \sum_{k=1}^{N_A^0} w(r_{jk})\right) \tag{4}$$

$$w(r_{jk}) = \frac{3}{2} \frac{1}{\tau_D} \kappa_{jk}^2 \left(\frac{R_0}{r_{jk}}\right)^6 \tag{5}$$

where τ_D is the unquenched donor lifetime. R_0 is the Förster radius for donor and acceptor pairs under the assumption of rapid dipole reorientation. We used the value $R_0 = 2.28$ nm determined previously.[10] Here, $w(r_{jk})$ is the rate of energy transfer between the jth donor and the kth acceptor separated by a distance r_{jk}, and κ_{jk}^2 is the orientation factor for this D−A pair.

According to eqs 4 and 5, the summation of $w(r_{jk})$ over the ensemble of donors and acceptors involves the product of a distance term (r_{jk}^{-6}) and a dipole orientation term κ_{jk}^2 for each D−A pair. These two parameters cannot be separated, and one can think of them as being "coupled". In a real system consisting of donor and acceptor ensembles, it is impossible to measure individual orientation factors for each D−A pair. As a consequence, a preaveraged orientation factor is normally used to simplify the FRET calculations. For a three-dimensional system with a random, homogeneous distribution of immobile donor and acceptor dyes, Baumann and Fayer have shown that $\langle|\kappa|\rangle^2 = 0.476$.[28] For FRET in systems with heterogeneous dipole distributions, the orientation factor may not have a preaveraged value. The MC methodology has the unique advantage that one can simulate the dipole orientation, as well as the dye loci, to calculate the individual orientation factor for each energy transfer D(j)−A(k) pair. This provides one with the opportunity to study the effect of individual dipole orientations on FRET kinetics.

As mentioned earlier, for block copolymers there is no reason to anticipate a correlation in the orientation of transition dipoles, and our simulations of block copolymer lamellae indicate that any correlation that exists is too small to be detected.[14] Thus, one is justified in assuming a random dipole distribution in computing donor decay profiles $I_D(t)$ from the ensemble of points generated in the MC calculation. Other simulations have shown that for donors and acceptors confined to thin Euclidean geometries (planar slabs, cylindrical shells) with a thickness on the order of R_0 FRET kinetics can be described by a preaveraged orientation term $\langle|\kappa|\rangle^2$ whose magnitude is somewhat smaller than 0.476.[13]

The experimental fluorescence decays were fitted with the averaged delta-function excitation decays calculated via eq 4 as described in refs 11 and 13. In the fitting process for each sample, we convoluted each of the delta-function excitation decays, calculated from the model with a certain assumed interface thickness value, with an instrument response ("lamp") function to generate a simulated experimental decay. This simulated decay was then used to fit the real experimental decay of the sample, employing a nonlinear least-squares algorithm. All fittings start from the third channel after the channel of maximum decay intensity. One measure of the goodness of the fit is the χ^2 parameter. For each sample, one obtains a χ^2 value for each assumed value of δ, and the optimized value of the interface width for each sample is given by the minimum value of χ^2 when plotted against assumed values of δ.

Results and Discussion

Lifetime Measurements on PI-9Phe−PMMA. Figure 3 shows the fluorescence decay of a film of neat Phe-labeled diblock copolymer. Fitting the decay with a single-exponential decay function gives a relatively high χ^2 value (1.40), a lifetime of 43.3 ns, and the weighted residuals and their autocorrelation show irregularities at early times. As expected, a double-exponential function gives a better fit ($\chi^2 = 1.20$ with randomly distributed weighted residuals and autocorrelation). It shows a second lifetime at 1.7 ns with a fraction of 2% and a main component with a lifetime of 43.4 ns.[29] As will be shown in the Supporting Information, the small fraction of short-lifetime component has no noticeable effect on the retrieved interface thickness if we assume that there is no energy transfer between the short-lifetime component and the acceptors.

Sample Morphology. Figure 4 shows the SAXS scattering intensity profiles (measured at room temperature) of the two individual diblock copolymers, for films annealed at 130 °C for 5 h. For both samples, ordered scattering peaks were observed with a pattern (1:$\sqrt{3}$:$\sqrt{4}$:$\sqrt{7}$...), clearly indicating that both polymer film samples are characterized by cylindrical morphologies. From ^{1}H NMR measurements we infer that the cylinder cores are composed of PI (29 vol %) in a PMMA (71

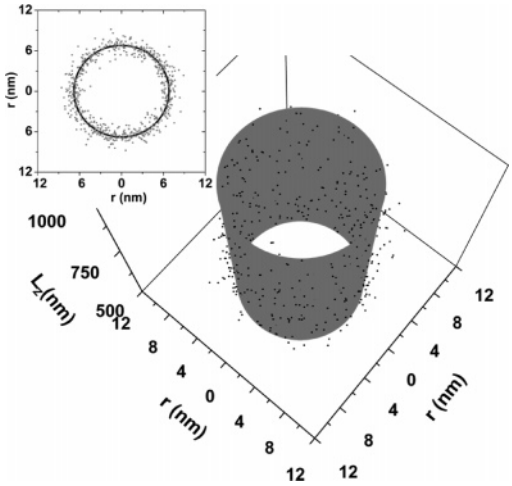

Figure 2. Three-dimensional spatial distribution of acceptors (scattered points, $C^0_{An} = 4.58$ mM) across a model of a diffuse cylindrical interface (thickness: 1.0 nm) constructed by the MC method. The dark tube (radius: 6.8 nm (r_{core}); length: $L_Z = 500$ nm) is the hypothetical "sharp" interface between the PI cylinder and the PMMA matrix. The length of the model interface along the tube direction (L_Z) is 500 nm. Periodic boundary conditions were employed in the vertical direction. The points refer to the loci of the centers of the transition dipoles of the dyes, and the simulation does not take into account the space-filling requirements of the polymer chains or the dyes. Inset: top view of the model system.

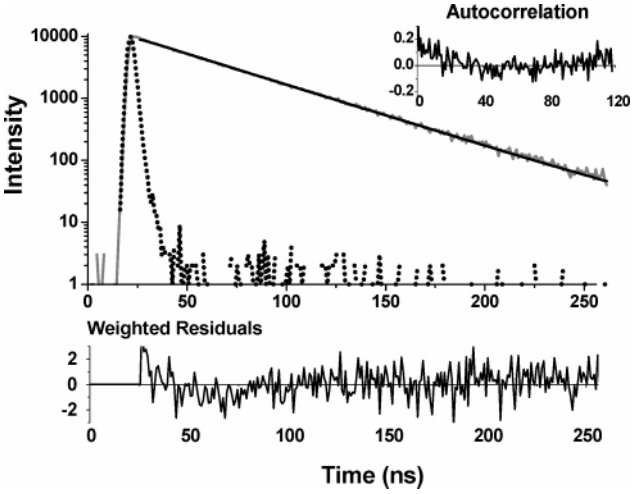

Figure 3. Fluorescence decay curve for a film of PI-Phe9−PMMA. The data were fitted (least-squares algorithm) by a single-exponential term (black line, lifetime 43.3 ns). The weighted residuals and autocorrelation function of the residuals are also shown, as an indication of the quality of the single-exponential fit ($\chi^2 = 1.40$). The dotted line is the instrument response function, measured by exciting a solution of *p*-terphenyl in deaerated cyclohexane (lifetime: 0.96 ns).

vol %) matrix. For both samples, the correlation distance between the PI cores calculated from the first scattering peak in the SAXS profile is 24 nm. We calculated the radius of the PI cylinder ($r_{core} = 6.8$ nm) on the basis of the volume fraction of PI.

Determination of Interface Thickness for PI−PMMA Cylinders. In this section, we apply the MC methodology to determine the width of cylindrical interface formed by the dye-labeled PI−PMMA samples. In this analysis, we neglect the weak short component in the $I_D(t)$ decay of the donor-labeled PI−PMMA and use $\tau_D = 43.3$ ns in our calculations.

Using a Preaveraged Orientation Factor Appropriate for Extended 3D Space. When one can legitimately employ a

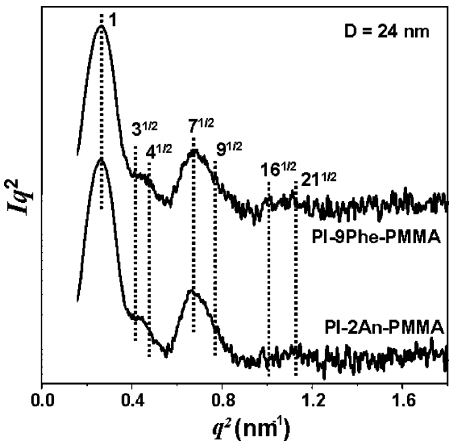

Figure 4. SAXS scattering curves for dye-labeled diblock copolymers PI-9Phe−PMMA and PI-2An−PMMA, as indicated in the figure. The film samples were annealed 5 h at 130 °C prior to the measurement. For each peak, the ratio of its position (q^2) to the first scattering peak position is shown.

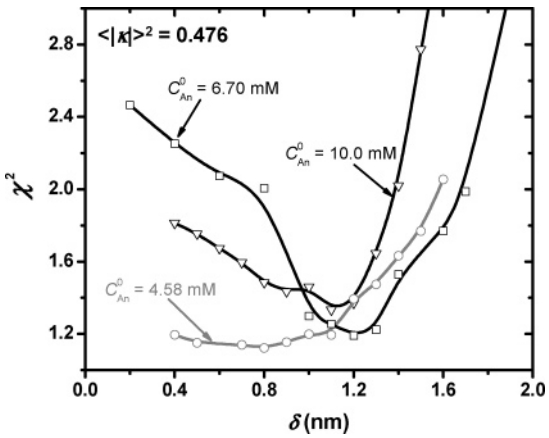

Figure 5. χ^2 plot for samples 2−4 listed in Table 2. The preaveraged orientation factor $\langle|\kappa|\rangle^2 = 0.476$ was used in the FRET calculations. The acceptor concentration for each curve is indicated in the figure.

preaveraged value of the orientation factor in a FRET calculation, eqs 4 and 5 can be rewritten as

$$I(t) = \frac{I_0}{N^0_D}\exp\left(-\frac{t}{\tau_D}\right)\sum_{j=1}^{N^0_D}\exp\left(-\frac{3}{2}\frac{t}{\tau_D}\langle|\kappa|\rangle^2\sum_{j=1}^{N^0_A}\left(\frac{R_0}{r_{jk}}\right)^6\right) \quad (6)$$

We begin by choosing the value of the orientation parameter ($\langle|\kappa|\rangle^2 = 0.476$) appropriate for rigid, randomly oriented dyes in extended three-dimensional space. This corresponds to the assumption we have made previously for data analysis for FRET measurements on lamellar block copolymer systems. For samples 2−4 in Table 2, we used eq 6 to calculate delta-function excitation decay profiles for each MC-generated dye distribution corresponding to different assumed values of the interface width. Then we followed the fitting procedure for the experimental decay profiles described in the previous section to construct plots of χ^2 values against the assumed δ value for each acceptor concentration. These plots are shown in Figure 5.

Figure 5 shows the χ^2 curves for the three samples with different acceptor concentrations. For the sample with the lowest acceptor concentration ($C^0_{An} = 4.58$ mM), values of δ much larger than 1.2 nm give poor fits, placing a reasonable upper limit on the interface width calculated with the assumption that $\langle|\kappa|\rangle^2 = 0.476$. For this sample, the goodness of fit is not very sensitive to the choice of δ in the range from 0.4 to 1.2 nm.

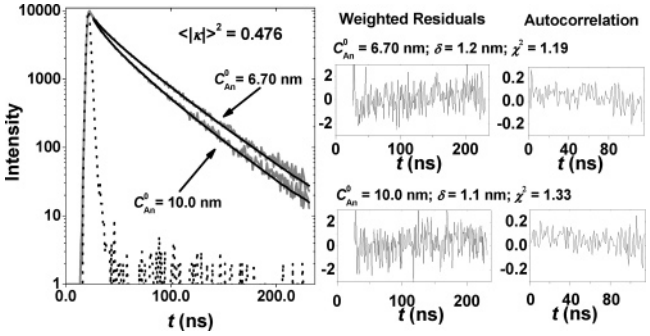

Figure 6. Left: fluorescence decay profiles from films of PI-9Phe−PMMA + PI-2An−PMMA copolymer mixtures annealed at 130 °C for 5 h. The dotted line is the instrument response function, obtained by exciting a solution of *p*-terphenyl in deaerated cyclohexane (lifetime: 0.96 ns). The black solid lines are the best fits of calculated fluorescence decays using eq 6 and the dye loci generated in the corresponding model systems. The acceptor concentrations are indicated in the figure. Right two columns: weighted residuals and autocorrelations of the "best" fits. χ^2 values for the nonlinear least-squares fitting and "optimized" interface thickness for each An concentration are indicated at the right side of the figure. In all calculations, we assumed a preaveraged orientation factor: $\langle|\kappa|\rangle^2 = 0.476$ (as is indicated in the figure).

The data analysis for the two higher acceptor concentrations (C^0_{An} = 6.70 and 10.0 mM) is more definitive and gives pronounced minima in the range of 1.1−1.2 nm. To emphasize how well the MC simulations are able to fit the data, we plot in Figure 6 the "best" fits (at the minimum of χ^2) of the experimental decays with simulated experimental decay profiles at these two different acceptor concentrations. The magnitude of χ^2 at the minimum of the χ^2 surface for the high concentration sample is somewhat larger than one expects for this type of experiment, but this is likely related to the presence of the weak short-lived component in the unquenched donor decay profile. At high acceptor concentration, a substantial fraction of the donor decay is "quenched" through FRET, making a short unquenched emission more prominent. When we performed a parallel set of FRET calculations by adding an additional short-lifetime term to eq 6 (or eq 4), we obtained a very similar χ^2 plot, but with a minimum value of $\chi^2 \leq 1.20$ (see the Supporting Information).

Assuming Random Dipoles. In the preceding section, we found that data analysis based upon a preaveraged value of $\langle|\kappa|\rangle^2 = 0.476$ for PI-9Phe−PMMA + PI-2An−PMMA blends with a cylindrical morphology led to a "best fit" interface width in the range of ca. 1.1−1.2 nm. This is very similar to the result ($\delta = 1.3 \pm 0.1$ nm) obtained for PI-9Phe−PMMA and PI-2An−PMMA lamellae also analyzed under the assumption that $\langle|\kappa|\rangle^2 = 0.476$.[10] The MC calculations allow one to examine the validity of this value for $\langle|\kappa|\rangle^2$ through a reanalysis of the same FRET data by assuming, for each D−A pair, randomly oriented rigid dipoles. When this type of calculation was applied to FRET data obtained for PI−PMMA lamellae, a somewhat smaller value of the interface width was obtained ($\delta = 1.0 \pm 0.2$ nm),[13] consistent with the idea that in restricted geometries characterized by a width on the order of $R_0/2$ the effective value of $\langle|\kappa|\rangle^2$ is somewhat smaller than 0.476.

When the donor fluorescence decay curves for samples 2−4 were reanalyzed by assuming that all dipoles had a random orientation, we obtained the χ^2 plots shown in Figure 7. In this analysis, the delta-function excitation fluorescence decays were calculated, using eqs 4 and 5, by considering individual orientation factors for each D−A pair.[30] Here, for all three acceptor concentrations, the χ^2 plots are rather flat for values of δ less than 1 nm. The interface width is found to be narrower than the value of 1.1 or 1.2 nm found using $\langle|\kappa|\rangle^2 = 0.476$. If one were to estimate a "best-fit" value for the interface width, it would be ca. 0.5−0.7 nm. As an indication of how well these simulated decay curves fit the measured donor decay profiles, we provide three examples (one for each sample concentration) in Figure 8. In each instance, the fit can be judged as excellent, except perhaps for the highest acceptor concentration, where the autocorrelation function is not entirely random.

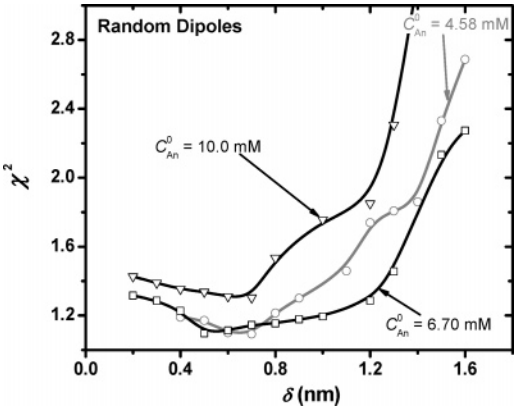

Figure 7. χ^2 plot for samples 2−4 listed in Table 2. We considered a random dipole orientation for individual D−A pairs in the FRET calculations. The acceptor concentration for each curve is indicated in the figure.

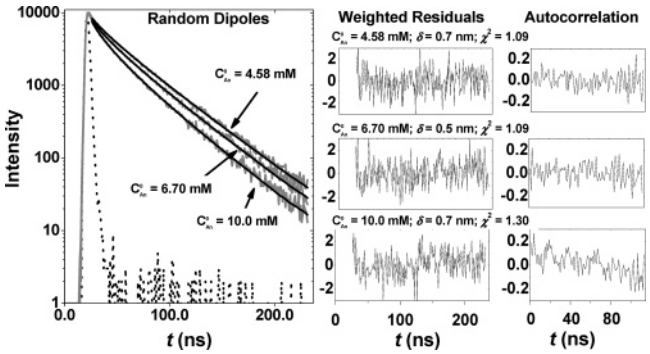

Figure 8. Fittings of the experimental fluorescence decays based on the assumption of random dipoles for individual D−A pairs. The decay curves presented correspond to the minima in the χ^2 plots in Figure 7. See Figure 6 for a further description of the contents of the figure.

Table 3. Preaveraged Orientation Factor $\langle|\kappa|\rangle^2$ Suggested for Cylindrical Shell Geometries for the Calculation of FRET Kinetics[a−c]

	$r_1 - r_2$				
r_1	$10R_0$	$3R_0$	R_0	$0.5R_0$	$0.25R_0$
$10R_0$	0.47	0.46	0.42	0.41	0.40
R_0			0.41	0.42	0.42

[a] r_1 = outer radius; $r_1 - r_2$ = shell thickness. [b] Taken from ref 13. [c] For $r_1 = 3R_0$ and $(r_1 - r_2) = 0.4R_0$, we found a "best-fit" value of $\langle|\kappa|\rangle^2 = 0.40$.

Choosing a More Appropriate Preaveraged Orientation Factor. Simulations of FRET experiments for donors and acceptors homogeneously distributed but confined to a thin cylindrical shell showed that the coupling between the orientation term and the D−A distance became important as the thickness of the shell became comparable in size to or smaller than R_0. These results of the simulations, reproduced in Table 3, show that FRET kinetics can be described effectively by a preaveraged orientation term, but its magnitude is smaller than that ($\langle|\kappa|\rangle^2 = 0.476$) appropriate for infinite three-dimensional

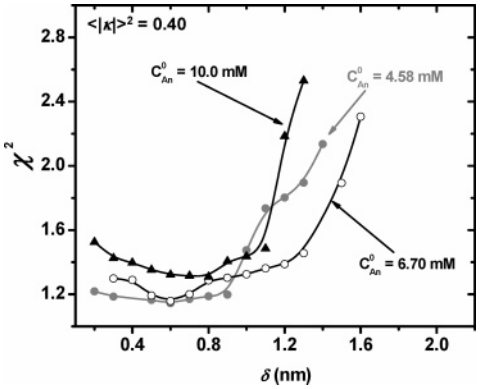

Figure 9. χ^2 plot for samples 2−4 listed in Table 2. We used a preaveraged orientation factor, $\langle|\kappa|\rangle^2 = 0.40$, in the FRET calculations. The acceptor concentration for each curve is indicated in the figure.

space.[13] As one can see in Table 3, the value of 0.476 is quite appropriate for a shell thickness as small as $3R_0$. The radius of the PI cylinders in the samples examined here is approximately $3R_0$ (6.8 nm/2.3 nm), and the interface thickness is on the order of 0.8 nm ($0.4R_0$). Because the example considered here does not correspond exactly to the systems listed in Table 3, we repeated the calculations for $r_1 = 3R_0$ and $(r_1 - r_2) = 0.4R_0$. For the latter situation, we found a "best-fit" value of $\langle|\kappa|\rangle^2 = 0.40$. When we reanalyze the experimental decay curves in terms of eq 6, using $\langle|\kappa|\rangle^2 = 0.40$, we obtain the χ^2 plots shown in Figure 9. These χ^2 curves are closer to those in Figure 7 for random dipoles than those in Figure 5 computed with $\langle|\kappa|\rangle^2 = 0.476$. The minima in the χ^2 curves lie roughly in the 0.6−0.8 nm range, close to the values obtained from the direct consideration of random dipoles.

A feature of these calculations that is not very satisfying is the absence of a strongly pronounced minimum in the χ^2 plots (as is seen for example for the curve for $C^0_{An} = 6.70$ mM in Figure 5) in all of the computations carried out for random dipoles and for $\langle|\kappa|\rangle^2 = 0.40$. This is different from what we found previously for simulations of the PI−PMMA lamellar geometry in ref 13, where there was clear indication of a best-fit value of the PI−PMMA interface of $\delta = 0.9 \pm 0.2$ nm determined by considering individual random dipole orientations and $\delta = 1.0 \pm 0.2$ nm for an appropriate preaveraged orientation factor. At least part of the difficulty is related to computational statistics. As mentioned above, we found considerable scatter when we tried to fit data with simulated fluorescence decay profiles generated from a single Monte Carlo calculation. We carried out five independent Monte Carlo calculations for each assumed interface width and each acceptor concentration, but we were obliged to average the five decays at each time channel to give an average decay, which was then used to fit the experimental decay.

Summary

In this paper, we examined the application of a Monte Carlo algorithm to fit experimental data obtained from FRET experiments on cylindrical structures formed by dye-labeled PI−PMMA samples. The construction of the model system was based on the actual sample morphology, as characterized by SAXS. The interface thickness between the PI core and PMMA matrix was retrieved from fitting simulated decays to the experimental fluorescence intensity decays and optimizing the fits. In the calculation of simulated donor fluorescence decays, we considered two cases of dipole orientation. In one case, we took specific pairwise account of individual random dipole orientations in the computation of simulated donor fluorescence decay profiles. In the other case, we introduced values of a preaveraged orientation factor $\langle|\kappa|\rangle^2$.

Our results showed that the value of interface thickness retrieved from the analysis of FRET decays depends on the way the dipole orientation is treated. For the cylindrical interface between PI and PMMA blocks, use of $\langle|\kappa|\rangle^2 = 0.476$ led to an interface width value of $\delta = 1.1-1.2$ nm. Pairwise consideration of random dipole orientations led to a smaller value of the interface width, in the range of $\delta = 0.5-1.0$ nm. This smaller value originates from the coupling between the dipole orientation and the D−A distance when dyes are confined to a narrow block copolymer interface with a width much smaller than R_0. A feature of the calculation that we still do not understand very well is why the χ^2 surface is much flatter, with much more poorly defined minima than the calculations based upon a preaveraged value of $\langle|\kappa|\rangle^2$. In addition, the minima, for various acceptor concentrations, are less well-defined than we found for corresponding experiments on dye-labeled PI−PMMA with a lamellar geometry.

On the basis of the results of previous simulations for donor and acceptor dyes distributed homogeneously in thin cylindrical shells with a thickness smaller than R_0, we anticipated that the experimental decays reported here could be fitted by assuming that $\langle|\kappa|\rangle^2 = 0.40$. Here we obtained the result that δ is about 0.6−0.8 nm. This value is smaller than (but within experimental error of) the value $\delta = 0.9 \pm 0.2$ nm determined by considering individual random dipole orientations for the width of the PI−PMMA lamellar interface.[13] While the polymer exhibiting the hexagonal phase, for which we obtain a somewhat thinner interface, has a slightly larger molar mass than the sample that forms lamellae, the molar mass difference is not significant in the context of Semenov's theory.[31]

These interfaces are very thin and represent the narrowest interfaces yet reported for a block copolymer system. It is not difficult to draw the conclusion that PI and PMMA are very meagerly miscible polymers.

Acknowledgment. The authors thank NSERC Canada and the ORDCF program of the Province of Ontario for their support of this research.

Supporting Information Available: Data analysis of experimental donor fluorescence decays by the Monte Carlo method, under the assumption that donor-labeled PI−PMMA has two lifetimes (1.7 and 43.4 ns). This material is available free of charge via the Internet at http://pubs.acs.org.

References and Notes

(1) Bates, F. S.; Fredrickson, G. H. *Annu. Rev. Phys. Chem.* **1990**, *41*, 525.
(2) Anastasiadis, S. H.; Russell, T. P.; Satija, S. K.; Majkrzak, C. F. *J. Chem. Phys.* **1990**, *92*, 5677.
(3) Russell, T. P.; Menelle, A.; Hamilton, W. A.; Smith, G. S.; Satija, S. K.; Majkrzak, C. F. *Macromolecules* **1991**, *24*, 5721.
(4) Shull, K. R.; Mayes, A. M.; Russell, T. P. *Macromolecules* **1993**, *26*, 3929.
(5) Ni, S.; Zhang, P.; Wang, Y.; Winnik, M. A. *Macromolecules* **1994**, *27*, 5742.
(6) Tcherkasskaya, O.; Ni, S.; Winnik, M. A. *Macromolecules* **1996**, *29*, 610.
(7) Yang, J.; Lu, J.; Rharbi, Y.; Cao, L.; Winnik, M. A.; Zhang, Y.; Wiesner, U. *Macromolecules* **2003**, *36*, 4485.
(8) Klafter, J.; Blumen, A. *J. Chem. Phys.* **1984**, *80*, 875.
(9) Yekta, A.; Duhamel, J.; Winnik, M. A. *Chem. Phys. Lett.* **1995**, *235*, 119.
(10) Yang, J.; Roller, R. S.; Winnik, M. A.; Zhang, Y.; Pakula, T. *Macromolecules* **2005**, *38*, 1256.
(11) Rharbi, Y.; Winnik, W. A. *Macromolecules* **2001**, *34*, 5238.

(12) Farinha, J. P. S.; Spiro, J. G.; Winnik, M. A. *J. Phys. Chem. B* **2004**, *108*, 16392.
(13) Yang, J.; Winnik, M. A. *J. Phys. Chem. B* **2005**, *109*, 18408.
(14) Yang, J.; Winnik, M. A.; Pakula, T. *Macromolecules* **2005**, *38*, 8882.
(15) O'Connor, D. V.; Phillips, D. *Time Correlated Single Photon Counting;* Academic Press: London, 1984.
(16) Yang, J.; Lu, J.; Winnik, M. A. *J. Polym. Sci., Part A: Polym. Chem.* **2003**, *41*, 1225.
(17) The syntheses and spectroscopic properties of model compounds were described in ref 16.
(18) Helfand, E.; Tagami, Y. *J. Chem. Phys.* **1972**, *56*, 3592.
(19) Helfand, E. *Macromolecules* **1975**, *8*, 552.
(20) Helfand, E.; Wasserman, Z. R. *Macromolecules* **1980**, *13*, 994.
(21) The point treatment assumes that there is no excluded volume associated with the dyes. We showed in ref 13 that this treatment led to no distortion in FRET calculations.
(22) This assumption holds true when the interface is narrow enough and the hexagonal cells are large enough—as in our case. For a very broad interface, one has to consider energy transfer from/to the neighboring hexagonal cells.
(23) The extent of energy transfer calculated from our methodology is independent of the donor concentration.
(24) For convenience, we set the origin at r_{core} (the radius of the dark sharp tube in Figure 2).
(25) Schmid, F.; Müller, M. *Macromolecules* **1995**, *28*, 8639.
(26) Yang, J.; Winik, M. A.; Pakula, T. *Macromol. Theory Simul.* **2005**, *14*, 9.
(27) Blumen, A.; Manz, J. *J. Chem. Phys.* **1979**, *71*, 4694.
(28) Baumann, J.; Fayer, M. D. *J. Chem. Phys.* **1986**, *85*, 4087.
(29) The fraction, f, was calculated based on $f = A_2\tau_2/(A_1\tau_1 + A_2\tau_2)$. The A_i and τ_i ($i = 1, 2$) are the coefficients and lifetimes of the double-exponential function $I(t) = A_1 \exp(-t/\tau_1) + A_2 \exp(-t/\tau_2)$.
(30) We chose three random numbers in the range −0.5 to 0.5. These three random numbers were used as the orientation vectors of a dipole in the *X*- ($\vec{x}$), *Y*- ($\vec{y}$), and *Z*-directions ($\vec{z}$). The unit vector of this dipole orientation $\vec{D}$ (or $\vec{A}$) can be expressed by $\vec{D} = (\vec{x},\vec{y},\vec{z})/\sqrt{\vec{x}^2+\vec{y}^2+\vec{z}^2}$, where $\sqrt{\vec{x}^2+\vec{y}^2+\vec{z}^2}$ is a normalization factor.
(31) Semenov, A. N. *Sov. Phys. JETP* **1985**, *61*, 733.

MA052068A